Using genetic algorithm-back propagation neural network prediction and finite-element model simulation to optimize the process of multiple-step incremental air-bending forming of sheet metal

Zemin Fu [a,*], Jianhua Mo [a], Lin Chen [b], Wei Chen [b]

[a] State Key Laboratory of Material Processing and Die & Mould Technology, Huazhong University of Science and Technology, Wuhan, 430074 Hubei, PR China
[b] SANY Heavy Industry Co. Ltd., Changsha, 410100 Hunan, PR China

ARTICLE INFO

ABSTRACT

Using neural network to predict punch radius based on the results of air-bending experiments of sheet metal is a high efficiency work in spite of little error. A three-layer back propagation neural network (BPNN) is developed to best fit this discrete engineering problem involving many parameters of air-bending forming. A genetic algorithm (GA) is used to optimize the weights of neural network for minimizing the error between the predictive punch radius and the experimental one. Then, with the predicted punch radius and other geometrical parameters of a tool, 2D and 3D ABAQUS finite-element models (FEM) are established, respectively. The original forming process of multiple-step incremental air-bending of sheet metal, obtained from geometric planning for semiellipse-shaped workpiece, is simulated using the FEM. This process is further adjusted with simulation-optimization results, because of existing large errors in the workpiece simulated with the original forming process. Finally, a semiellipse-shaped workpiece, with average errors of +0.61/−0.62 mm, is manufactured with the optimized adjustment process. The experimental results show that the punch design method is feasible with the prediction model of GA-BPNN, and the means of optimizing process with FEM simulation is effective. It can be taken as a new approach for punch and process design of multiple-step incremental air-bending forming of sheet metal.

© 2009 Elsevier Ltd. All rights reserved.

1. Introduction

Air-bending (Fig. 1) is performed with a punch and a die with a pair of shoulders. The die gap is set according to the process requirements, and the sheet metal is placed on the shoulders. The punch at the mid-span of the die is given a displacement, and the die is deep enough to avoid the sheet from striking its bottom. This single-step air-bending processing is suitable for workpieces of simple profile. However, parts with complex surface can not be bent by the single-step air-bending. To solve this problem, a multiple-step incremental air-bending forming is utilized. This forming process is a flexible sheet-metal-forming technology that uses principles of stepped manufacturing. It transforms the complicated geometry information into a series of parameters of single-step, and then the plastic deformation is carried out step by step through the computer numerical controlled movements of the punch and sheet feed for getting the desired part. Therefore, the process is cost-effective to form large complex parts in small to medium batches such as semiellipse-shaped workpieces which could be used as crane boom, tele-

scopic arm of the concrete pump truck, boom of bridge, and petroleum piping.

Air-bending springback is unavoidable in the sheet metal forming, and the springback leads to the changes of bending radius, bending arc segment and bending angle. The bending radius of a sheet metal after unloading is called springback radius; the bending arc segment of a sheet metal after removal from the punch is defined as springback arc segment; the unloaded bend angle is referred as springback angle (Fig. 1). Due to the existence of springback, the precision of products and subsequent assembly operations were severely affected. How to effectively control springback angle and springback radius has been the key issue to precision forming and design of air-bending punch. We note that many methods have been proposed to control springback angle. Overbending through a deeper punch stroke is one of the commonly used methods to control springback angle in air-bending. However, overbending has a minor influence to springback radius. Therefore, in order to accurately control springback radius, a nonlinear prediction model of punch radius, taking springback radius as the model input, is established in this paper.

As punch radius, as the output of the non-linear model, is too difficult to be calculated exactly by table checking and experience, artificial neural network happens to map the non-linear
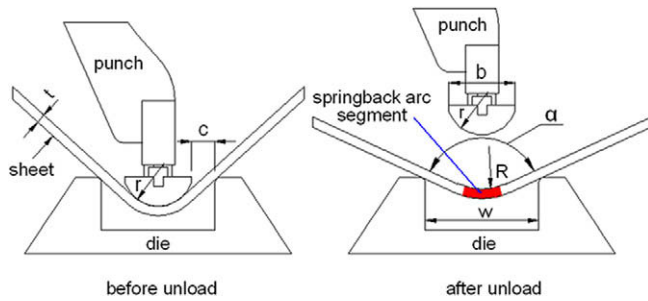

Fig. 1. Geometrical model of air-bending of sheet metal (R, springback radius; α, springback angle; c, tool gap; r, punch radius; t, sheet thickness, σ, yield strength; w, die width; b, punch width; E, Young's modulus).

relationship [1]. It provides a new way to solve the complex, non-linear, polytropic, discrete engineering problem involving in many parameters of air-bending forming. In recent years, much work has been investigated on the application of BPNN (back propagation neural network) for optimizing the forming process, for tool wear monitoring, and for parameter diagnose [2–4]. However, BPNN is prone to getting into local extreme and convergence is slow. To overcome these drawbacks, this study attempts to combine GA (genetic algorithm), avoiding local minima and achieving global convergence quickly and correctly by searching in several regions simultaneously, with BPNN to minimize the total mean squared error (MSE) between actual output of the network and the desired output through optimizing the weights of neural network.

There are two main aspects to apply GA into BPNN [5], as follows: one is to optimize the weights of the network, and the other is to optimize the topological structure of the network. The former will be discussed in this paper. The learning process of network is considered as the dynamic process for continuous optimization of the weights and thresholds. GA is an optimization and search technique based on the principles of genetics and natural selection. GA has remarkable abilities which include being able to solve non-smooth, non-continuous, non-differentiable fitness functions, to escape the local optima and acquire a global optimal solution. Therefore, this research intends to establish a prediction model of punch radius with GA-BPNN, and check its applicability from the view point of making the production process more efficient.

Though there are literatures on the FEM simulation of sheet metal single-step air-bending forming [6,7], little is reported on that of the multi-step air-bending forming. In order to reduce the number of forming experiments, it is important to study multi-step incremental air-bending forming with FEM simulation method to obtain the optimized process parameters of workpiece-forming.

In the present paper, punch design and FEM simulation of multiple-step incremental air-bending forming were taken as the subject investigated. First, based on the tests for air-bending of sheet metal, a prediction model of punch radius is developed with GA and BPNN. Second, a punch is designed according to the developed model, geometric planning of multi-step incremental-forming process is performed, the incremental-forming process planned with

geometry is simulated, and this process is furtherly corrected with FEM simulation-optimization. Finally, a semiellipse-shaped workpiece with 11,528 mm × 764 mm × 583 mm is machined with the simulation-optimization results. In the following paper, the validity and practicality of the above work will be further proved.

2. Punch radius model

The air-bending forming process involves various parameters, such as the material property, geometric parameters of sheet metal, tool topological structure, tool gap, punch displacement, and friction. The springback radius is affected by these parameters, the influence degree is various. On the base of experimental verification and orthogonal test analysis, the four most significant influential factors are considered here: punch radius (r), sheet thickness (t), yield strength (σ) and Young's modulus (E; Fig. 1).

However, other parameters with comparatively minor influence on springback radius, like normal anisotropy, strain hardening exponent, sheet length, friction, punch displacement, tool gap, etc., are ignored. Therefore, springback radius (R) is related to the four factors (r, t, σ and E). In other words, the model of punch radius (r), taking R, t, σ and E as independent variables, can be presented in

$$r = \psi(R, t, \sigma/E) \tag{1}$$

2.1. Test for single-step air-bending of sheet metal

2.1.1. Test condition
The utilized sheet metal properties are shown in Table 1. URSVI-KEN OPTIMA 2200-ton press brake is used for air-bending tests of the sheet metal, the tool gap (c) between the punch and the die is 20 mm (Fig. 1), and the punch displacement is 45 mm in each test. The formed workpieces are measured with the Atos-II three-dimensional laser scanning system with a ±0.005 mm precision.

2.1.2. Test results
At first, the forming tests are designed with the test parameters of r, t, and σ/E. Then, 68-set tests are done under different material properties and process parameters. Lastly, the 3D point cloud data of the formed workpiece is obtained with the Atos-II three-dimensional laser measuring system. The point cloud data is transferred into the CAD/CAM software for modeling. Springback radius of the formed workpiece can be obtained from the CAD model. The 68 sets of springback radius data and test parameters are shown in Table 2. They will be used as the training and testing samples of BP network detailed in Section 2.3.

2.2. Establishing the punch radius model with GA and BPNN

2.2.1. BPNN prediction model for punch radius
2.2.1.1. Neural networks. Artificial neural networks are a large class of parallel processing architectures, which can mimic complex and non-linear relationships through the application of many non-linear processing units called neurons. The relationship can be

Table 1
Material properties.

Material	E (MPa)	σ (MPa)	Poisson's ratio	Density (kg/m^3)	σ/E
WELDOX700-1	217069.7	776.287	0.266	7830	0.00358
WELDOX900-2	200405.4	956.009	0.276	7830	0.00477
Q235A	206378.3	239.783	0.3	7850	0.00116
WELDOX700-2	178846.6	699.842	0.243	7830	0.00391
WELDOX900-1	205856.3	950.812	0.284	7830	0.00466

Table 2
The results of air-bending test.

Sample case	r (mm)	t (mm)	σ/E	R (mm)
S1	25	6	0.0039	26.32
S2	60	9	0.0048	66.51
S3	193	7	0.0012	215.52
S4	60	6	0.0039	68.1
S5	142	6	0.0012	155.41
S6	70	8	0.0036	77.44
S7	193	8	0.0046	290.37
S8	50	7	0.0039	54.68
S9	70	6	0.0012	73.17
S10	100	6	0.0048	131.82
S11	60	8	0.0036	65.41
S12	193	6	0.0039	310.81
S13	25	8	0.0036	26.01
S14	193	9	0.0048	280.15
S15	70	9	0.0048	78.98
S16	25	9	0.0012	25.33
S17	70	6	0.0039	81.24
S18	142	8	0.0048	191.28
S19	70	7	0.0036	78.62
S20	193	6	0.0046	349.08
S21	100	8	0.0012	104.76
S22	25	7	0.0012	25.41
S23	50	9	0.0036	53.31
S24	70	8	0.0046	79.77
S25	142	9	0.0046	181.95
S26	70	8	0.0012	72.38
S27	193	8	0.0012	211.58
S28	50	8	0.0048	55.07
S29	70	7	0.0046	81.38
S30	142	7	0.0036	182.27
S31	60	8	0.0046	67.06
S32	70	9	0.0012	72.12
S33	25	6	0.0046	26.6
S34	142	8	0.0039	179.62
S35	193	7	0.0048	321.58
S36	60	7	0.0046	68.2
S37	25	8	0.0046	26.21
S38	193	9	0.0036	251.77
S39	142	6	0.0039	196.97
S40	100	7	0.0046	124.85
S41	50	6	0.0048	56.94
S42	100	9	0.0036	113.78
S43	25	9	0.0046	26.11
S44	70	9	0.0039	77.15
S45	142	6	0.0046	211.64
S46	193	8	0.0039	269.7
S47	50	9	0.0046	54.27
S48	70	6	0.0048	84.34
S49	142	7	0.0048	201.24
S50	193	6	0.0012	218.56
S51	100	6	0.0012	106.5
S52	142	8	0.0012	151.85
S53	50	8	0.0012	51.24
S54	142	9	0.0012	150.7
S55	50	6	0.0012	51.56
S56	100	9	0.0046	118.33
S57	142	9	0.0036	171.5
S58	193	9	0.0012	209.35
S59	60	7	0.0012	62.01
S60	100	7	0.0036	118.43
S61	25	7	0.0036	26.11
S62	60	6	0.0048	70.26
S63	142	7	0.0012	153.36
S64	60	9	0.0012	61.57
S65	100	8	0.0039	117.27
S66	70	7	0.0012	72.72
S67	50	7	0.0046	55.59
S68	193	7	0.0036	275.71

Fig. 2. Architecture of three-layer BPNN for punch radius prediction.

mely useful in recognizing patterns in complex data. The resulting quantitative models are transparent; they can be interrogated to reveal the patterns and the model parameters can be studied to illuminate the significance of particular variables [10].

Hormik et al. [11] has proved a three layered feed-forward neural network with back propagation algorithm can map any non-linear relationship with a desired degree of accuracy. In this paper, a three layer back propagation network (Fig. 2) is developed to predict punch radius, where the transfer functions in hidden and output layer are sigmoid and linear, respectively. The three parameters (R, t, σ/E) in Eq. (1) are the input to the BPNN, the punch radius (r) in Eq. (1) is the output of the network. The number of hidden layer is fixed to 7 by trail, which is detailed in Section 2.2.1.2. Then a network model with 3-7-1 architecture is established (Fig. 2).

As shown in Fig. 2, $IW_{1,1}$ is the weight from the input to the hidden layer, $LW_{2,1}$ is the weight from the hidden layer to the output layer, b_1 is the weight of the bias unit added to the hidden layer, b_2 is the weight of the bias unit added to the output layer, a_1 is the output in the hidden layer, a_2 is the actual output of the network, and p_1 is the net input.

During the BP network learning process, the error is subsequently backward propagated through the network to adjust the weights of the connections and threshold, minimizing the sum of the mean squared error (MSE) in the output layer,

$$U = \frac{1}{2} \sum_{k=1}^{G} \sum_{j=1}^{m} [T_j(k) - Y_j(k)]^2, \qquad (2)$$

where U is the sum of the mean squared error, m is the number of output nodes, G is the number of training samples, $T_j(k)$ is the expected output, and $Y_j(k)$ is the actual output.

The parameters used for BPNN are as follows: maximum epochs 4000, momentum constant 0.8, learning rate 0.02, and expectation error of network 0.0001.

2.2.1.2. Overfitting. It should be noted that a potential difficulty with the use of powerful non-linear regression methods is the possibility of overfitting data. In the above developed model, to avoid this difficulty, the experimental data are divided into two sets, a training dataset and a testing dataset. The model is produced using only the training data. The testing data are then used to check that the model behaves itself when presented with previously unseen data [10]. In addition, the proper selection of the number of neurons in the hidden layer can avoid the overfitting of neural network effectively.

After different neuron numbers in the hidden layer are tried, when the number is 7, the mean absolute error of the training data and testing data is at a minimum, which is shown in Table 3. It is easy to find that when the number is 13, the training errors are very small while testing errors are quite big. Thus, the overfitting phenomenon of the network is obvious. Figs. 3 and 4 show that

'learned' by a neural network through adequate training from the experimental data [8]. Artificial neural network provides a parameterized, non-linear mapping between inputs and outputs. It has the inherent capability to deal with fuzzy information, whose functional relations are not clear [9]. Neural networks are clearly extre-
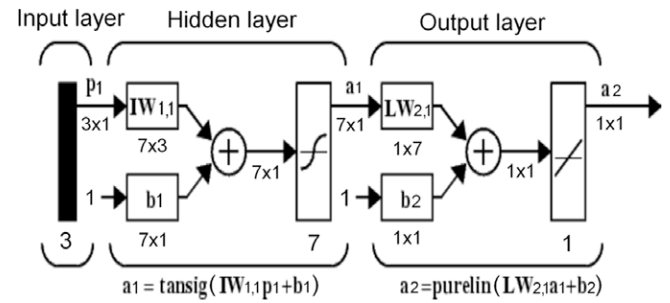
Table 3
Comparison of mean absolute error using different number of neurons in hidden layer.

Number of neurons in hidden layer	Mean absolute error of training data	Mean absolute error of testing data
3	0.0938	0.2634
5	0.0621	0.1376
7	0.0225	0.1014
9	0.0358	0.6488
11	0.0614	0.351
13	0.0564	2.7948
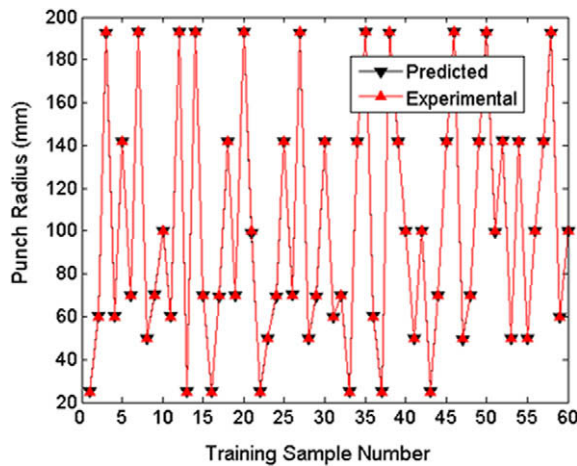
Fig. 3. Comparisons between predictive values and actual values for training samples.
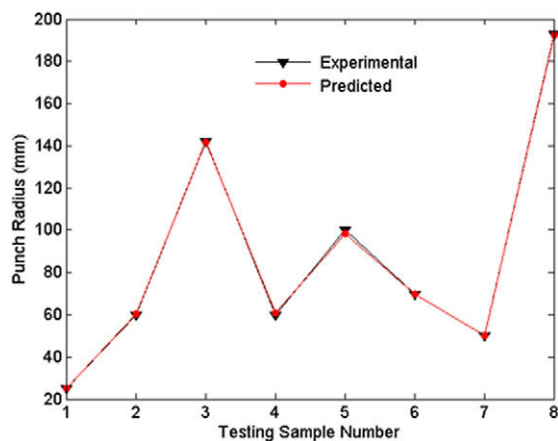
Fig. 4. Comparisons between predictive values and actual values for testing samples.

training errors and testing errors are very small when the neuron number is 7. This means that this network finds out the best compromise between predictability and overfitting if the neuron number is 7 in the hidden layer. Hence, a network with one hidden layer consisting of 7 hidden neurons is the optimal configuration for the prediction of punch radius for multiple-step incremental air-bending forming of sheet metal.

2.2.2. BPNN based on GA

2.2.2.1. Fitness function and genetic operation of GA. GA has been proved to be capable of finding global optima in complex problems

by exploring virtually all regions of the state space and exploiting promising areas through mutation, crossover and selection operations applied to individuals in the populations [12]. It applies selection, crossover and mutation operators to construct fitter solutions. A genetic algorithm processes the populations of chromosomes by replacing unsuitable candidates according to the fitness function. In this study, the fitness function is the average deviation between expected and predicted values of punch radius (r). The fitness value of a chromosome is calculated using the total mean squared error of the BPNN architecture. A fitness value F is given by

$$F = \frac{1}{U+1} \tag{3}$$

where U is the sum of the mean squared error given by Eq. (2). Thus, the smaller the network's total mean squared error, the closer a fitness value to 1 (maximum) [12]. Once fitness values of all chromosomes are evaluated, a population of chromosomes is updated using three genetic operators: selection, crossover and mutation. The three operators are described as follows:

The selection operator of genetic algorithm is implemented by using the roulette-wheel algorithm to determine which population members are chosen as parents that will create offspring for the next generation. Crossover is a mechanism of randomly exchanging information between two chromosomes. The paper uses arithmetical crossover which can ensure the offspring are still in the constraint region and moreover the system is more stable and the variance of the best solution is smaller. Mutation operation can change the values of randomly chosen gene bits, and this process continues until some pre-defined termination criteria are fulfilled. Mutation operation aims to make genetic algorithm obtain

Table 4
The comparison of the GA-BPNN model and BPNN.

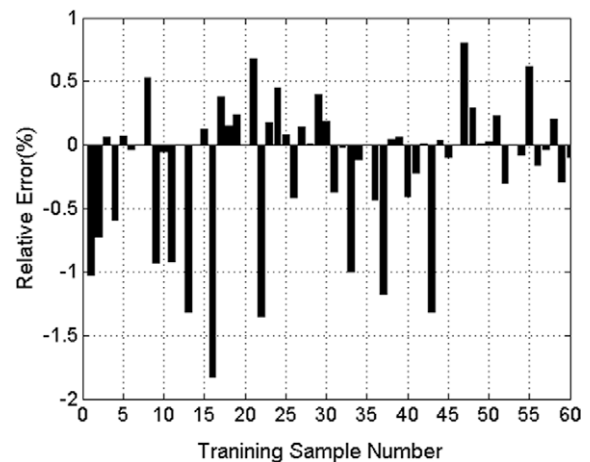| Randomly extract from sample case	Experimental punch radius r (mm)	GA-BPNN model		BPNN model	
		r	δ (%)	r	δ (%)
S37	25	24.65	1.40	26.12	4.48
S23	50	50.33	0.66	52.32	4.64
S59	60	59.56	0.73	57.84	3.60
S6	70	70.68	0.97	74.11	5.87
S40	100	99.28	0.72	96.37	3.63
S30	142	143.20	0.84	147.55	3.91
S54	142	142.65	0.46	147.79	4.08
S14	193	193.63	0.32	188.34	2.41

Fig. 5. Training error.

local random research capability through varying certain genes of chromosome.

The parameters used for GA are as follows: population size 80, termination generation 120, length of chromosome 30 bits (10 bits for each parameter), crossover probability 0.8, mutation probability 0.03.

2.2.2.2. Optimization with genetic algorithm. A GA allows a population composed of many individuals to evolve under specified selection rules to a state that maximizes the fitness values (*F*) in Eq. (3). The objective of the optimization is to maximize the fitness values (*F*) which would lead to the minimization of the total mean squared error (*U*) from Eq. (2). This makes the ideal prediction results of the BPNN be obtained.

As seen in Eq. (2), the minimizing process of *U* value is the adjusting and optimizing process of weights and thresholds of the BPNN. Therefore, the GA is used to optimize the weights and thresholds of the BPNN. It is the weights optimization that is addressed in the current work.

2.2.2.3. BPNN learning based on GA optimization. The BPNN learning process consists of two stages: firstly employing GA to search for optimal or approximate optimal connection weights and thresholds for the network, then using the back-propagation learning rule and training algorithm to adjust the final weights. The operations are as follows:

The BPNN weights and thresholds ($IW_{1,1}$, $LW_{2,1}$, b_1, b_2) are initialized as genes of chromosome, and then the global optimum is searched through selection, crossover and mutation operators of genetic algorithm. This procedure is completed by applying a BP algorithm on the GA established initial connection weights and

thresholds. If the BP network's total mean squared error is bigger than the expected error, the weights and thresholds will be updated; otherwise, they are saved as initial value of BP network training. After that, they are further adjusted under BP learning rule to the best results, by which the punch radius (*r*) can be accurately predicted.

2.3. Training and testing the GA-BPNN model

Input–output data for the GA-BPNN training and testing are from the test results of air-bending. Sixty sets of data (from S1 to S60) at Table 2 are used to train the neural network model, and the others (from S61 to S68) are utilized to test the network model.

As the dimension and magnitude of original sample data are different, the input data and test data should be normalized before training. That is:

$$X_i' = 2 \times \frac{X_i - X_{\min}}{X_{\max} - X_{\min}} - 1 \tag{4}$$

Implementation procedure of the network training is programmed within the Matlab environment using GA and Neural Networks Tool Boxes.

2.4. Results and analysis

While using the optimized neural network model to predict the punch radius, the comparisons between predictive values and actual values for training samples are shown in Fig. 3. And the comparison of results from the predictive values of testing samples which do not participate in training network and actual values of them is shown in Fig. 4.
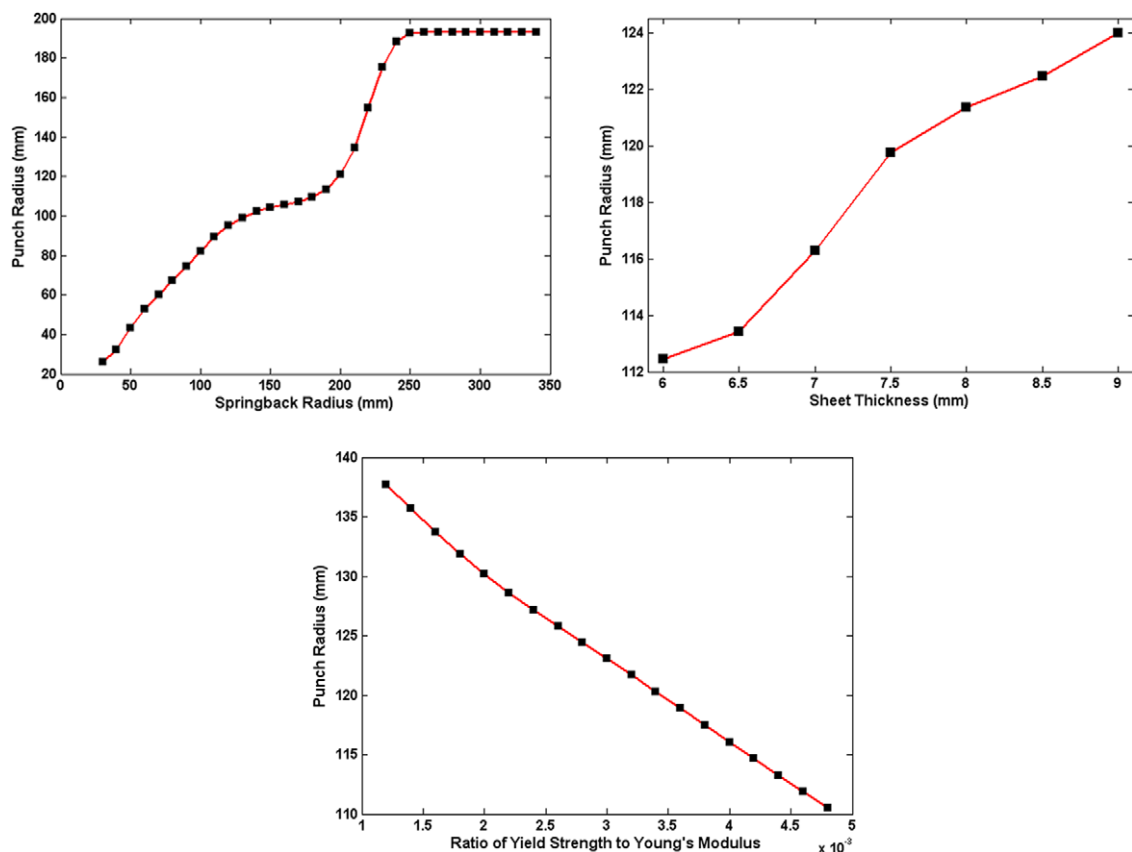

Fig. 6. Relationships between various process parameters and punch radius.

The relative error (%) of training network is shown in Fig. 5.

As can be seen from the figures, the punch radii predicted by the GA-BPNN model are very close to the actual experimental data. The prediction results of the GA-BPNN model are shown in Table 4. Compared to the BPNN model, the relative error of GA-BPNN model is much lower than the BPNN model. So the conclusion can be drawn that the proposed GA-BPNN model has more accurate prediction ability. Based on that, we attempt to solve the punch radius, as key geometric parameter for tool design of air-bending forming, with the GA-BPNN model.

The relationships between various process parameters and punch radius are studied by using the GA-BPNN model (see Fig. 6).

The springback radius is found to be the significant influencing factor on punch radius. For air-bending of sheet metal, the punch radius can be reduced by selecting those materials with bigger yield strength, smaller Young's modulus and thinner sheet metal, which can be taken as a reference for designing punch.

3. Punch design with the GA-BPNN model

The section of the first arm of one crane telescopic boom is designed (Fig. 7), the workpiece length is 11,528 mm, which is made from WELDOX 900-1 (Table 1).

Since the length of the workpiece neutral plane is constant before and after springback, the incremental-forming process can be planned according to geometric shape and size of the workpiece
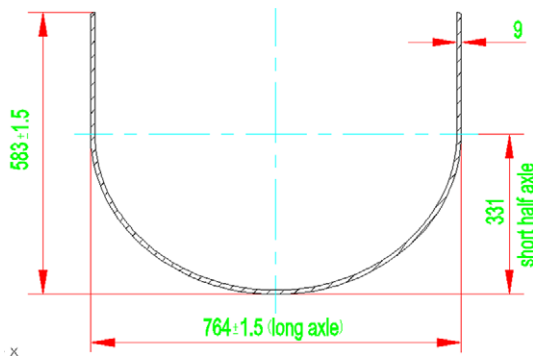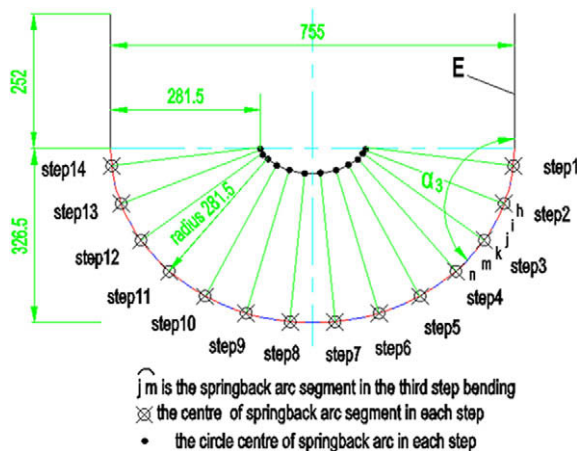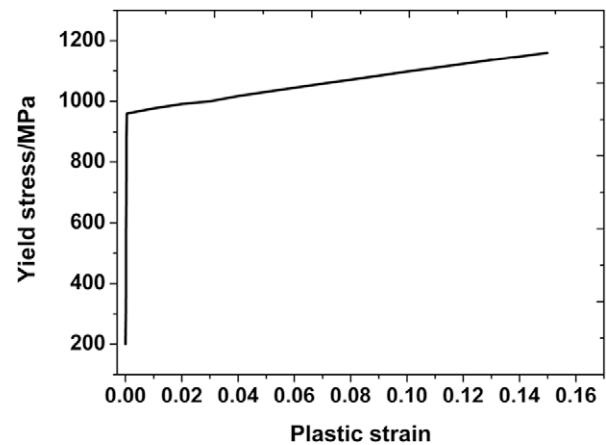

Fig. 9. Stress–plastic strain curve of WELDOX900-1 sheet.

neutral plane (Fig. 8). The workpiece is to be bent through 14 steps. The circle center of the springback arc in each step ensures to be on the small semiellipse, and the center of springback arc segment in each step ensures to be on the big semiellipse. The developed length for two adjacent center points of springback arc segments is regarded as sheet feed rate. For example, the developed length of *hk* (Fig. 8) is the sheet feed rate in the third step bending. The angles between line *E* and the tangent lines of *ij*, *mn*, ... are regarded as springback angle in each step bending after unloading, for instance, the angle α_3 is the springback angle in the third step bending after unloading. The biggest offset between the two concentric semiellipse is 281.5 mm, which can make springback arc
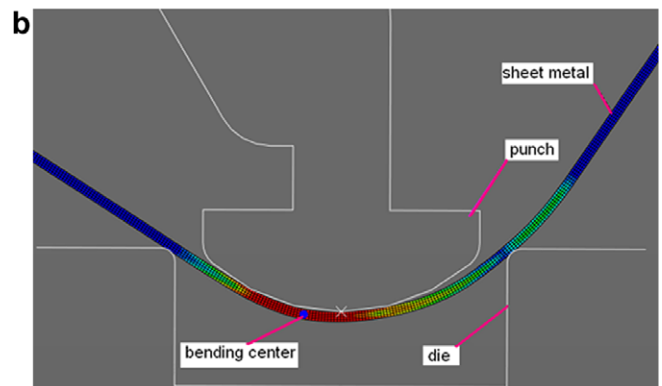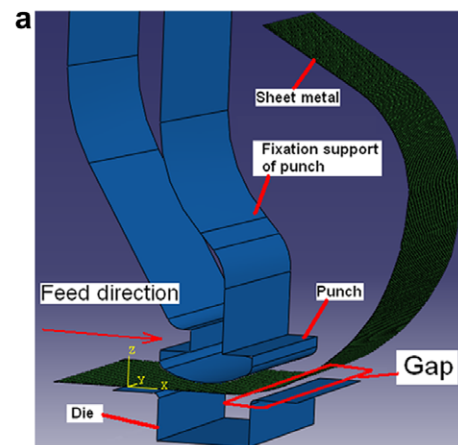

Fig. 7. Semiellipse-shape workpiece.

Fig. 8. Process planning of 14-step incremental air-bending forming of the first arm.

Fig. 10. FEM model of incremental air-bending forming process: (a) before bending and (b) bending.

Table 5
The results from experiments and simulations for single- and multiple-stroke air-bending.

Punch displace (mm)	Springback angle (α) obtained with experiments			Springback angle (α) obtained with simulations			Difference between experiment results of multiple stroke and simulation results of single stroke
	Single stroke	Multiple stroke	Difference	Single stroke	Multiple stroke	Difference	
25.45	178.33	178.17	0.16	178.23	178.21	0.02	0.06
28.69	174.69	174.47	0.22	174.61	174.59	0.02	0.14
32.02	169.58	169.27	0.31	169.49	169.48	0.01	0.22
35.19	162.98	162.88	0.10	162.90	162.88	0.02	0.02
38.65	152.83	152.70	0.13	152.76	152.75	0.01	0.06

All angles in degrees.

segment in each step to be the most ideal curve approximating semiellipse.

Therefore, the springback radius $R = 281.5 - t/2 = 281.5 - 4.5 = 277$ mm in each step, it is taken as the input of neural network, punch radius (r) is output ten times continuously with this prediction model, and the optimized weight and threshold each time were used as initial value of the next network training. Thus, the punch radii (r) of 192.575 mm, 192.715 mm, 192.685 mm, 192.812 mm, 192.830 mm, 192.931 mm, 192.981 mm, 192.979 mm, 192.936 mm, 192.999 mm could be obtained, respectively. The average value is 192.844, that is $r = 193$ mm through rounding, which will be utilized to establish finite-element model in Section 4.2 as well as to manufacture punch in Section 5.

4. FEM simulation for workpiece-forming

To reduce the number of experiments for multiple-step incremental air-bending forming of sheet metal, process parameters have to be optimized with numerical simulation.

4.1. Simulation algorithm

The multiple-step incremental air-bending forming of sheet metal is an extremely complicated physical process. It is a high non-linear problem including geometric non-linear, material non-linear and contact non-linear. To solve this, the explicit algorithm of ABAQUS/Explicit module fitted for dynamic and non-linear analysis could be used to simulate the sheet metal forming process, and the implicit algorithm of ABAQUS/Standard module adapted to static and steady analysis to simulate the springback process.

Due to the result of any time during the ABAQUS/Standard module running can be treated as initial condition run in the ABAQUS/Explicit module for further calculating and analyzing, and vice versa. Therefore, ABAQUS software function is very suitable for multiple-step air-bending process. We integrate ABAQUS/Explicit and ABAQUS/Standard to carry out the mixed operations. This method can make the non-linear behavior of each step in multiple-step air-bending forming be solved with higher precision and faster convergence, compared with algorithms of other FEM software.

4.2. Simulation setup

4.2.1. Material and process parameters

The sheet metal with 11,528 mm × 1612 mm × 9 mm dimensions are made from WELDOX 900-1 (Table 1), and its property curve of the stress–plastic strain is shown in Fig. 9.

The punch pressing speed of 8 mm/s is chosen according to the operating requirements of URSVKEN 2200-ton press brake, and the mass scaling factor is set as 10. The punch radius of 193 mm ($r = 193$ mm) is obtained from the prediction model, and then the

punch width of 200 mm ($b = 200$ mm) and the die width of 240 mm ($w = 240$ mm) (Fig. 1) are determined. The number of air-bending steps is 14. Sheet feed rate and springback angle of each step are obtained from the geometric planning of incremental air-bending forming process (Fig. 8).

4.2.2. Finite-element model

A three-dimensional finite-element model (Fig. 10a), only considering sheet with 500 mm length due to having the same cross section in length direction, is established for the multiple-step incremental air-bending forming process. The sheet metal was meshed with 15,819 nodes and 5160 elements (ABAQUS type CPS8R, namely the eight-node biquadratic plane stress quadrilateral, reduced integration shell elements). Its material is assumed to be planar anisotropic following Hill yield criterion. The punch and die are modeled as rigid surfaces. Coulomb friction principle is applied with a friction coefficient of 0.12 between the sheet, and the punch and die. The contact condition is implemented
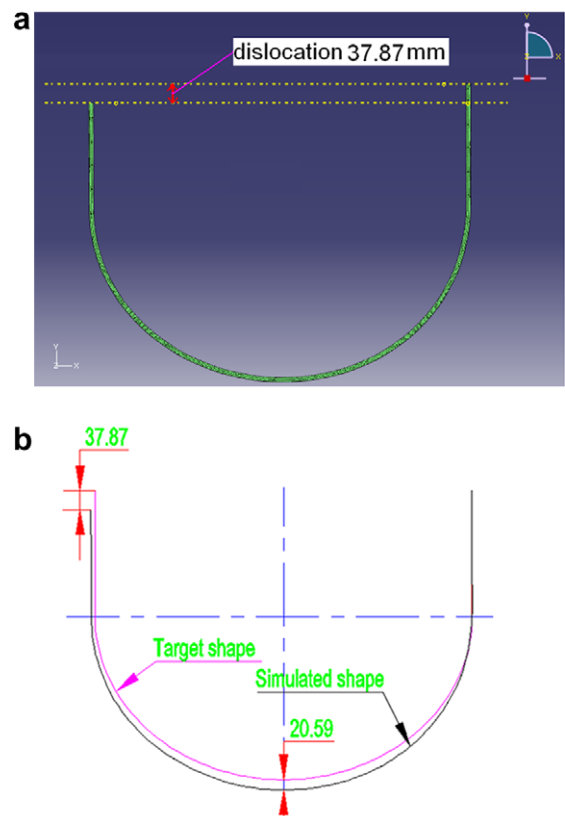

Fig. 11. Simulation results for semiellipse-shaped workpiece before optimization: (a) the simulated workpiece with the forming process of geometric planning, (b) shape errors in neutral layer between the target workpiece and the simulated one.

through a pure master–slave contact-searching algorithm and penalty contact force algorithm. To improve the calculation efficiency and facilitate analysis, the 2D FEM model is established for the process, as shown in Fig. 10b.

4.3. Forming simulation for a semiellipse-shaped workpiece of sheet metal

4.3.1. Simulation of both single- and multiple-stroke air-bending in single-step air-bending forming

In the practical forming, it is difficult to accurately obtain the required springback angle of sheet metal parts after forming with only single-stroke bending. We note that it needs multiple-stroke to complete air-bending operation of single-step. However, in simulation with FEM, the desired springback angle can be obtained with single-stroke air-bending. In order to arrive at the same

effect in using multiple-stroke bending needed in the practical forming and single-stroke bending in simulating forming, it is desirable to demonstrate that the number of loading–unloading cycles does not have a significant influence on the springback behavior of the material. Wang et al. [13] has verified that the stress–strain history and the release of residual stress prior to the final stroke have a negligible effect on the final unloaded bend angle by using the experiments and finite element analyses, respectively. However, in literature, the results from experiments and simulations cannot be contrasted and analyzed. Therefore, it is necessary for the results of their comparison analyses to be further discussed for simulating forming of multiple-step air-bending more effectively.

To contrast the differences of the springback angle between single-stroke and multiple-stroke incremental bending processes, experiments and finite element analyses are conducted. The tool-
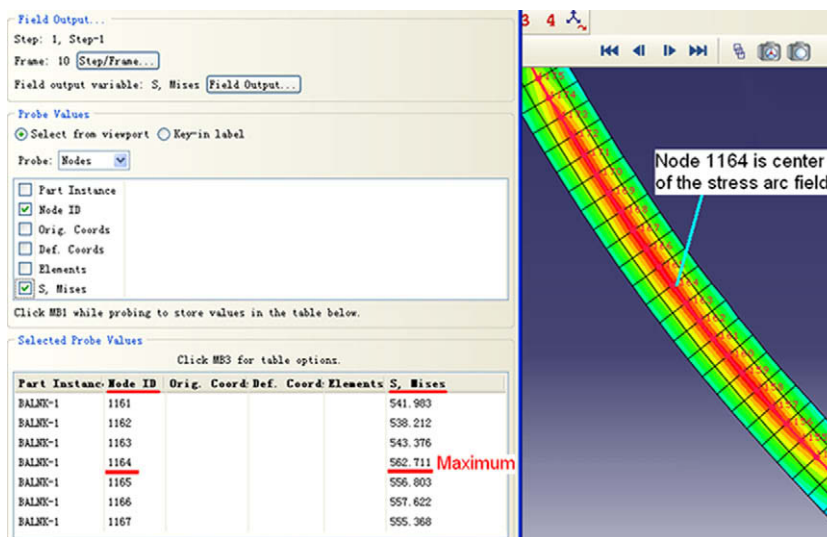

Fig. 12. Residual stress field of the formed shape with sheet feed rate of 73 mm in second step.
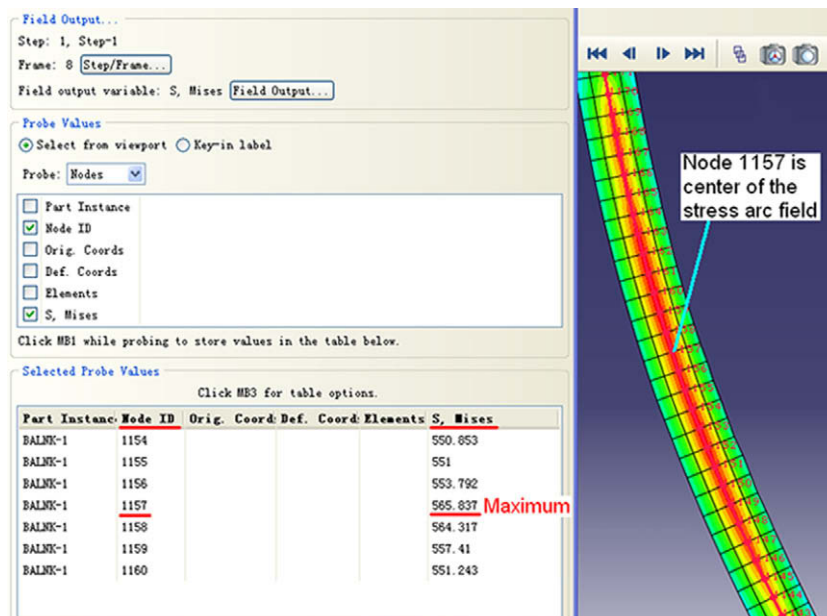

Fig. 13. Residual stress field of the formed shape with sheet feed rate of 49.8 mm in second step.

ing geometry and material data for the experiments are given in Section 4.2.1. Five final punch positions are used in the experiments and simulations. For multiple-stroke bending operations, three increments/strokes are used to reach the final punch positions. As can been seen from Table 5, the average differences in springback angels between single- and multiple-stroke processes, based on two groups of experiment and simulation, are 0.18° and 0.016°, respectively, and the average differences between experiment results of multiple-stroke bending and simulation re-

sults of single-stroke bending are small (just 0.1°). This shows that single-stroke air-bending process can be used to equivalently simulate multiple-stroke incremental bending process needed in the practical forming. Moreover, it is also demonstrated that simulation process is very close to practical forming process.

4.3.2. Simulation for multiple-step incremental air-bending forming process of geometric programming

The geometry data of the semiellipse-shaped workpiece are transformed into 14 single-step parameters, such as the sheet feed rate and springback angle of each step in Fig. 8. These parameters are used in simulation to form this workpiece. To ensure the reality of the simulation, firstly, the difference in springback angles between the simulated and the desired, adjusted by controlling the time-step size set up in explicit algorithm module, should be less than 0.02°. And the error of sheet feed rate should be within 0.1 mm. Secondly, residual stress, produced in the workpiece by each step bending after unloading, cannot be omitted in simulation process. Finally, under consideration of the interference between the workpiece and the fixation support of punch as well as the increasing holding force from the deadweight of the workpiece, the air-bending processing sequence needs to be largely adjusted according to the simulation analysis and theory calculation. The optimum sequence can be arranged as: from step 1 to step 7, step 14, step13, step 12 to step 8 (Fig. 8).

Fig. 11a shows the simulation results of semiellipse-shaped workpiece formed with the process from geometric planning. The target shape in the workpiece neutral layer and the simulated one are shown in Fig. 11b. It is clear that there exists the bigger error caused by distortion and dislocation of the simulated workpiece. Therefore, this process needs to be further optimized by adjusting the simulation parameters.

4.3.3. Optimization of process parameters with simulation

The reason causing the forming errors in Fig. 11b is that one end of the sheet metal touched with the die shoulders is line-segment-shape, while the other one without touching the shoulders is arc-segment-shape (Fig. 10a), which leads to offset of the bending center when loaded (Fig. 10b). This makes the centers of the arc-shaped residual stress fields in simulation do not coincide with the centers of springback arc segments in geometric programming. Therefore, In order to form workpiece with high-dimensional precision, the sheet feed rate in each step needs to be adjusted accurately so that the corresponding centers from the simulated and the planned can coincide (Fig. 14b). For example, sheet feed rate for the second step obtained by the 2D CAD is 73 mm, the geometric center of arc segment is located at node 1157. While the simulation results show that center of the arc-shaped residual stress field is located at node 1164 (Fig. 12). The two centers are not coincident and the error is 21.7 mm. Therefore, the sheet feed rate needs adjustment. In simulation, we note that when the sheet feed rate is 49.8 mm, the center of the arc-shaped residual stress field is located at node 1157 (Fig. 13), the two center points are identical. The sheet feeding quantities of other steps can be optimized by the same way as the second step.

In Fig. 10a, when sheet metal is moved in the opposite feed direction, the sheet feed rate is smaller and the gap is bigger. In other words, the smaller the sheet feed rate is, the bigger the gap is and the more the overlap area between the punch and workpiece arc segment formed by the last step is; and much more overlap area can bring smoother surface of the workpiece and higher precision shape. Therefore, the number of air-bending steps is set as much as possible to achieve smaller sheet feed rate when we do the process planning. However, we should choose the optimum number of air-bending steps, which takes the production efficiency
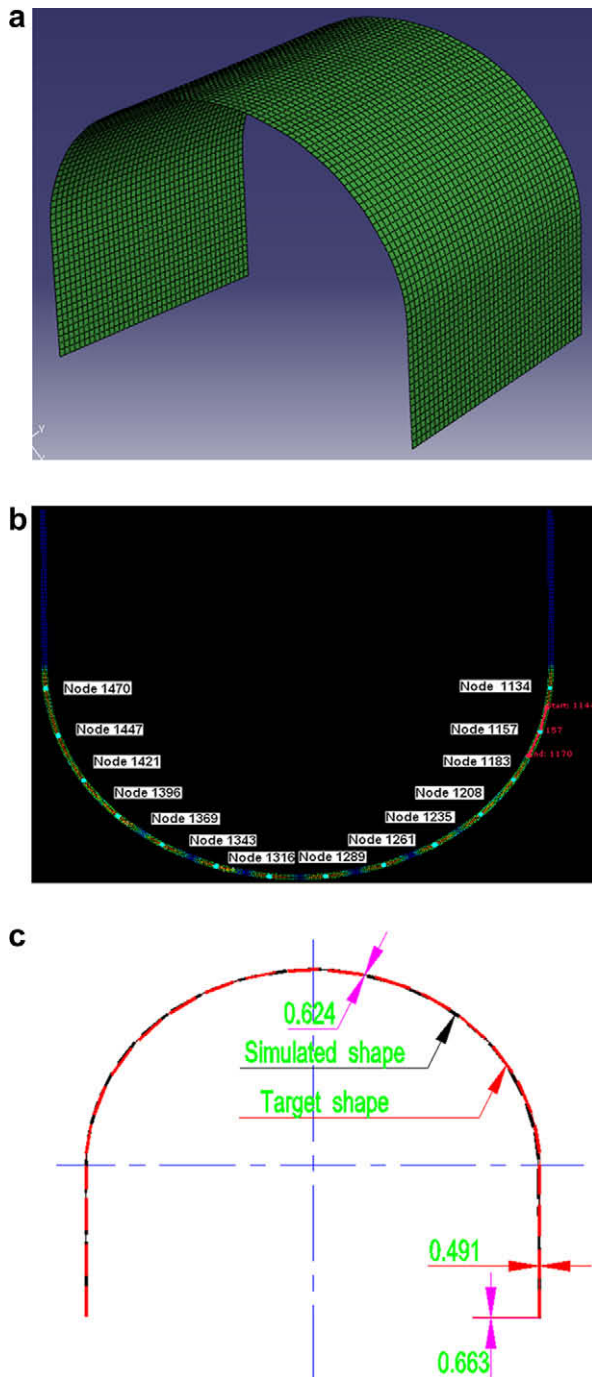

Fig. 14. Simulation results for semiellipse-shaped workpiece after optimization: (a) the simulated workpiece with the optimization process, (b) Nodes' residual stress centers coinciding with centers of springback arc segments in geometric planning, (c) shape errors in neutral layer between the target workpiece and the simulated one.

of workpiece-forming, product accuracy, and process simplification into consideration as well.

Fig. 14a shows the simulation results of 3D semiellipse-shaped workpiece formed with the optimized process. 2D residual stress fields and their centers in each step simulated by the optimized process can be observed in Fig. 14b. The target curve in the workpiece neutral layer along with results from the simulation-optimization method are shown in Fig. 14c. Obviously, after optimization, the forming error of the workpiece becomes negligible. The simulated shape is nearly identical to the desired target. As a result, the high-dimensional precision of the formed workpiece is obtained by simulation-optimization.

5. Application examples

A new punch is manufactured with the above study results. Then, a semiellipse-shaped workpiece (Fig. 15) is formed at the

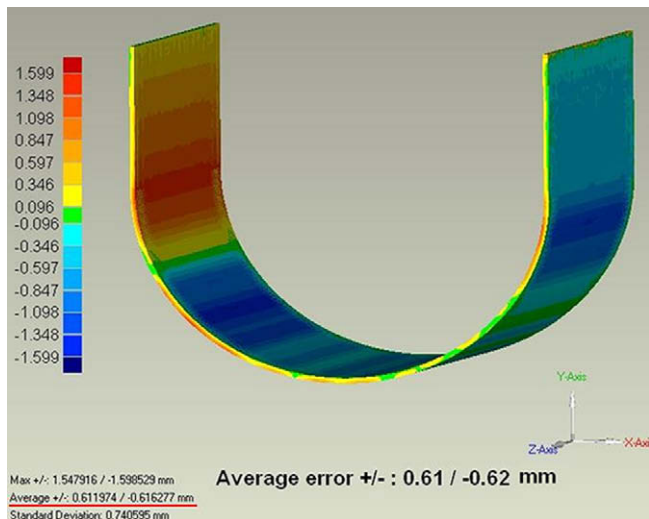**Fig. 15.** The first arm formed at the URSVKEN 2200-ton press brake.

Fig. 16. Matching result of measured point cloud model of the cut one with 500 mm length from the scanned part and CAD model.

URSVIKEN 2200-ton press brake with the punch and the process data from the simulation-optimization in Section 4.3.3.

The surface profile of the workpiece is measured with Atos-II three-dimensional laser measuring system, and a 3D point cloud model is obtained. The 3D point cloud model is matched with CAD model with Geomagic Qualify software, and the results show that the average dimension errors of the part are +0.61/−0.62 (Fig. 16), which meets the requirements of workpiece form and position accuracy.

6. Conclusions

The prediction model of punch radius in sheet metal air-bending forming is constructed by using GA-BPNN and testing technique in this paper. Then, the multiple-step incremental air-bending forming process of sheet metal is optimized with FEM simulation method. The present work predicted and designed the punch, built FEM model, and simulated and machined a semiellipse-shaped workpiece. From the above discussion, the following conclusions can be made:

(1) The genetic algorithm is adopted to optimize the weights and thresholds of neural network. The established GA-BPNN model is capable of accurate prediction on punch radius with less time and faster convergence, which can provide optimum parameters for punch design.
(2) The simulation of single-stroke air-bending, which is equivalent to multiple-stroke air-bending needed in practical forming process, can be used to improve simulation precision and efficiency.
(3) The simulation-optimization method has been confirmed by experiment to be capable of providing optimum process parameters for multiple-step incremental air-bending forming, which has been successfully applied in manufacturing of one semiellipse-shaped workpiece used in crane boom.
(4) The manufacturing results show that these methods of punch design and FEM simulation-optimization for multiple-step incremental air-bending forming of sheet metal is reasonable and effective.

References

[1] Liu WJ, Liu Q, Ruan F, Liang ZY, Qiu HY. Springback prediction for sheet metal forming based on GA-ANN technology. J Mater Process Technol 2007;187–188:227–31.
[2] Yao YX, Li XL, Yuan ZJ. Tool wear detection with fuzzy classification and wavelet fuzzy neural network. Int J Mach Tools Manuf 1999;213:1525–38.
[3] Liao TW, Chen LJ. Manufacturing process modeling and optimization based on multi-layer perceptron network. J Manuf Sci Eng 1998;120:109–19.
[4] Wang L, Lee TC. Prediction of limiting dome height using neural network and finite element method. Int J Adv Manuf Technol 2006;27:1082–8.
[5] Whitfield D, Martin EH. New directions in cryptography. IEEE Trans Inform Theory 1986;14–15:644–54.
[6] Math M, Grizelj B. Finite element approach in the plate bending process. J Mater Process Technol 2001;125–126:778–84.
[7] Esat V, Darendeliler H, Gokler ML. Finite element analysis of springback in bending of aluminum sheets. Mater Design 2002;23:223–9.
[8] Lin YC, Zhang J, Zhong J. Application of neural networks to predict the elevated temperature flow behavior of a low alloy steel. Comput Mater Sci 2008;43(4):752–8.

[9] Mandal S, Sivaprasad PV, Dube RK. Modeling microstructural evolution during dynamic recrystallization of alloy D9 using artificial neural network. J Mater Eng Perform 2007;16(6):672–9.

[10] Bhadeshia HKDH. Neural networks in materials science. ISIJ Int 1999;39:966.

[11] Hormik K, Stinchhcombe M, White H. Multilayer feedforward networks are universal approximators. Neural Netw 1989;68:359–66.

[12] Hardalac F. Classification of educational backgrounds of students using musical intelligence and perception with the help of genetic neural networks. Expert Syst Appl 2009;36:6708–13.

[13] Wang J, Verma S, Alexander R, Gau JT. Springback control of sheet metal air bending process. J Manuf Process 2008;10(1):21–7.